

# Bursty Transport in Tokamaks with Internal Transport Barriers

S. Benkadda 1), O. Agullo 1), P. Beyer 1), N. Bian 1), P. H. Diamond 3), C. Figarella 1), X. Garbet 2), P. Ghendrih 2), V. Grandgirard 1), Y. Sarazin 2)

1) CNRS – Université de Provence, Marseille, France

2) Association EURATOM – CEA, St. Paul-lez-Durance, France

3) University of California, La Jolla, CA

e-mail contact of main author: benkadda@up.univ-mrs.fr

**Abstract.** Large scale transport events are studied using two different three dimensional simulation codes related to resistive ballooning and ion temperature gradient turbulence. The turbulence is driven by a constant incoming flux. In the case of resistive ballooning simulations, the underlying structures are found to be radially elongated at the low field side, and distorted by magnetic shear in parallel direction (streamers). The non linear character of these structures is emphasized. Bursty transport is investigated in presence of zonal flows and internal transport barriers generated either by a strong shear flow or with a magnetic shear reversal. Finally, a low dimensional model that captures the main features of bursty transport dynamics is derived.

## 1. Introduction

Recently, many self-consistent – in the sense that neither spatial nor time scale separability between the fluctuations and the equilibrium is assumed – fluid models of threshold plasma turbulence have shown that the radial transport exhibits intermittent ballistic bursts corresponding to large radial scale transport events [1, 2, 3, 4, 5, 6]. Also, experimental measurements of tokamak turbulence show evidence of intermittent transport [7, 8], together with scale invariance in time of the fluctuations [9]. They might be good candidates to explain fast transients [10]. A single structure of this sort is suggested to be a radially extended, poloidally localized convective cell called a streamer [11, 12]. Let us emphasize that this bursty transport is observed in systems driven at constant flux. In the present study, this flux driven turbulence is investigated with a 3-D global code of ion temperature gradient turbulence [13, 1] and with a 3-D global code computing resistive ballooning modes which involve a critical pressure gradient length [3]. These codes yield a consistent description of transport processes from the small scale fluctuations to the equilibrium profiles. Several issues are addressed here: the 3-D structure of the radially elongated large scale transport event (streamer) and its non linear character; the influence of zonal flows on the dynamics of these structures, the role of internal transport barriers (ITB) generated either by a strong shear flow or with a magnetic shear reversal on these transport events; and finally we derive a low dimensional model that captures the essential of the dynamics of the bursts.

## 2. Identification and characterization of large scale transport events

We use simulations of resistive ballooning turbulence at the plasma edge to investigate the three dimensional structure of the bursts. The turbulence is driven by a constant incoming flux. The model consists of two equations for the vorticity and pressure, respectively. The

normalized form of these equations is [14, 15]

$$\frac{d}{dt}\nabla_{\perp}^2\phi = -\nabla_{\parallel}^2\phi - Gp + \nu\nabla_{\perp}^4\phi, \quad (1)$$

$$\frac{dp}{dt} = \chi_{\parallel}\nabla_{\parallel}^2p + \chi_{\perp}\nabla_{\perp}^2p + S. \quad (2)$$

Here,  $d/dt = \partial/\partial t + \{\phi, \cdot\}$ , where the Poisson bracket represents the convection due to the  $\vec{E} \times \vec{B}$  flow. Note that the aim of this work is to study basic dynamic processes in 3D turbulence at the plasma edge. Therefore, in this simplified MHD model, diamagnetic effects and magnetic fluctuations are not included. Eqs. (1,2) describe the evolution of the complete fields of potential and pressure, including equilibrium and fluctuations. Expanding the fields  $\phi$  and  $p$  into Fourier series in the poloidal (mode number  $m$ ) and toroidal ( $n$ ) directions, each Fourier mode is localized in the vicinity of its resonant surface  $x = x_{q=m/n}$ . The simulation region is restricted to the domain between the  $q = 2$  and  $q = 3$  surfaces at the plasma edge.

Following the time evolution of the radial pressure profile, large bursts are observed alternating with quiet periods, as illustrated in Fig. 1. One observes both low pressure events traveling inwards and high pressure bursts propagating in the outward direction. Note that the early times shown in Fig. 1 correspond to a transient phase where the mean pressure gradient has not yet reached a statistically stationary state. In this phase, many large bursts are observed. From Fig. 1, it is possible to determine a time when a large burst appears. To investigate the 3D structure of this burst, the spatial distribution of the turbulent radial flux is analyzed at that specific time. A dominant structure corresponding to a strong local maximum of the flux is observed. At the low field side, this structure is highly elongated in the radial direction which suggests its interpretation as a streamer.

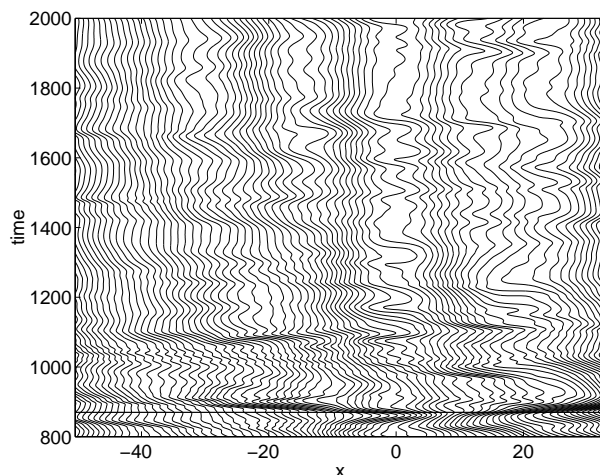


Figure 1: *Time evolution of the magnetic surface averaged pressure profile (isobars in the  $(x, t)$ -plane). In this case, zonal flows are suppressed.*

To illustrate this, Fig. 2 shows the contours of the turbulent radial flux in a small section of the poloidal plane, at the toroidal position where the structure passes at the low field side. In the toroidal direction, the maximum of the flux follows the local magnetic field line at each radial position, which results in a strong distortion due to magnetic shear. This

indicates that structures and magnetic shear are not incompatible. Since the modulational structure drive has ballooning character, the streamer can adjust to the magnetic shear.

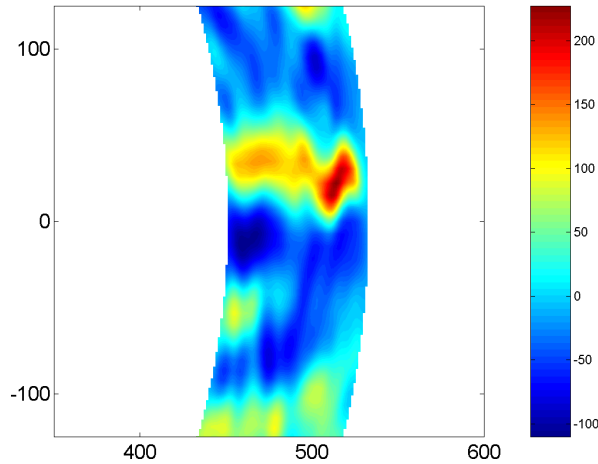


Figure 2: *Radially elongated structure (streamer) of the turbulent radial flux in a section (at the low field side) of a poloidal plane.*

To distinguish between a possible linear or nonlinear character of the structure, the toroidal wavenumber spectrum of the corresponding kinetic energy is calculated and plotted in Fig. 3. It shows that the streamer is composed of a large ( $\sim 10$ ) number of modes with different toroidal wavenumbers  $n$  and is therefore clearly different from a linear ballooning mode that is characterized by a single wavenumber  $n$  [16]. Therefore, there is a strong evidence that the generation of streamers is an intrinsically multimode nonlinear process rather than a secondary instability of a purely linear eigenmode flow.

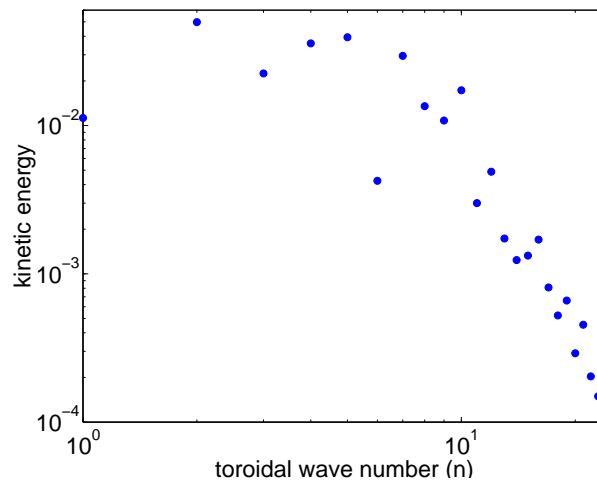


Figure 3: *Kinetic energy of the fluctuations as a function of the toroidal wavenumber, at the same time as in Fig. 2*

### 3. Interplay of zonal flows with streamers

In the previous simulations, the generation of zonal flows has been artificially suppressed. In order to study the influence of these flows on the large scale transport events, simulations including self consistently generated zonal flows are performed. The frequency of appearance of bursts is found to be remarkably higher compared to the previous case

(Fig. 1). On the other hand, the amplitudes of single events are lower. More precisely, the spectrum of the turbulent radial flux at a given radial position exhibits a  $1/f$  decrease in a range of intermediate frequencies [17, 1, 2] up to a certain cutoff, and the latter is extended to higher frequencies when zonal flows are included. This behavior can be understood analyzing the time evolution of the velocity shear at the same given radial position. When a burst is building up, the velocity shear starts growing after a short time delay, inhibiting the flux to grow to large amplitudes. This is due to the decorrelation of the radially elongated structures by the shear stress (Fig. 4). The cross correlation function of the turbulent radial flux and the velocity shear shows a maximum at a time delay of the order of 20 time units. This corresponds roughly to the cutoff in the frequency spectrum mentioned above.

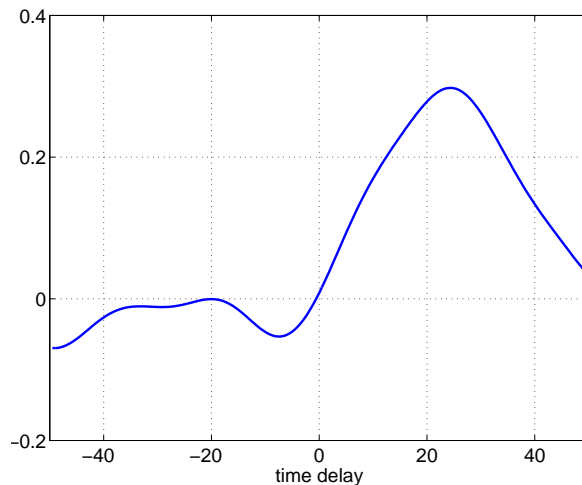


Figure 4: *Cross correlation between the radial turbulent flux and the velocity shear at a given radial position.*

The change in the frequency spectrum is in perfect agreement with the one observed in Ref. [18] in the running sandpile model. There, a suppression of the low-frequency components and an increase of the high-frequency parts are observed. Here, the simulations presented so far confirm the increase at high frequencies in the presence of zonal flows. As will be shown now, the decrease at low frequencies is due to a region with strong mean shear that is investigated in Ref. [18].

#### 4. Bursty transport with internal transport barriers

An interesting question is the behavior of the large scale events in presence of an ITB. It was postulated that a strong shear flow should prevent the propagation of such events [19, 17, 18]. Therefore, a simulation is performed, imposing a sheared equilibrium rotation at the vicinity of the  $x = 0$  surface. The velocity shear is five times larger than those generated by the turbulence in the previous simulation. In this case, a transport barrier builds up in the shear region, characterized by a strongly reduced turbulent radial flux (Fig. 5).

Bursts are still observed in this region, but their amplitudes are very small, and coming from both sides of the barrier, they almost vanish in the center. However, some perturbation travel through the barrier, as shown by recent simulations [20]. The frequency of appearance of bursts is even higher than in the previous case. In fact, the reduction of

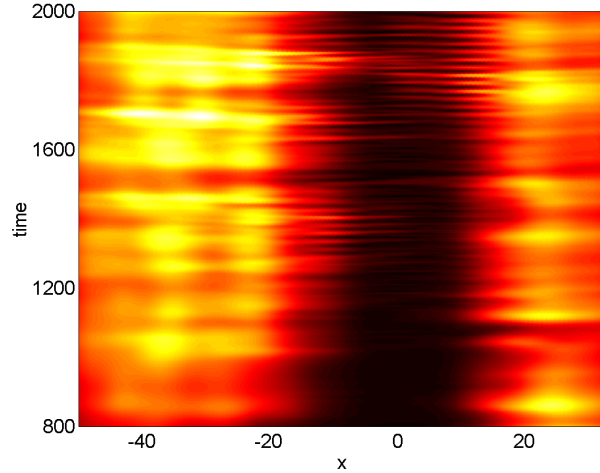


Figure 5: *Time evolution of the magnetic surface averaged turbulent radial flux in the case with externally imposed strong shear flow [minimum = -0.1 (black), maximum = 3.8 (white)].*

turbulent transport is found to be due to the suppression of low frequency components in the turbulent flux. As the time averaged total radial flux is constant, the transport in the barrier region must be approximatively neoclassical. In fact, a large pressure gradient builds up in this region. Note that the character of the bursts inside the barrier is close to that of a quasi-coherent oscillation.

Furthermore, ITG simulations show that with a magnetic shear reversal, an internal transport barrier builds up together with a strong ExB shear flow (Fig. 6). This supports the idea that within an ITB, turbulence is suppressed by a combination of EXB shear flow and a magnetic shear.

It is observed in this case that the events hardly cross an ITB. This is consistent with a shearing by the ExB flow in the barrier. Let us note that the biggest events do cross the barrier. However the frequency power spectrum of the turbulent flux exhibits the same shape inside and outside the ITB while only the amplitudes of the events change. This seems to differ from the previous case of resistive ballooning turbulence where the barrier was produced with an externally driven velocity profile. The reason seems that there are still bursts inside the barrier although their amplitude is low. The interplay between bursts outside and inside the ITB is still under investigation, Let us note that the barrier width also exhibits a complex behavior and that it is probable that zonal flows do affect this dynamics.

## 5. Low dimensional model for bursty transport

We propose a one dimensional (1-D) simplified model to investigate transport in turbulent systems driven by a fixed flux. We use a Galerkin projection to derive a low dimensional system that accounts for the dynamical properties of the bursts. This model relies on the possibility of generation of a mean poloidal ExB velocity field and its back reaction on fluctuations. In the present model, the production of this mean shear flow is a direct consequence of turbulence-induced Reynolds stress. The model is inferred from a 2-D interchange turbulence (equivalent to the resistive ballooning in the region located after the last closed magnetic surface) [4].

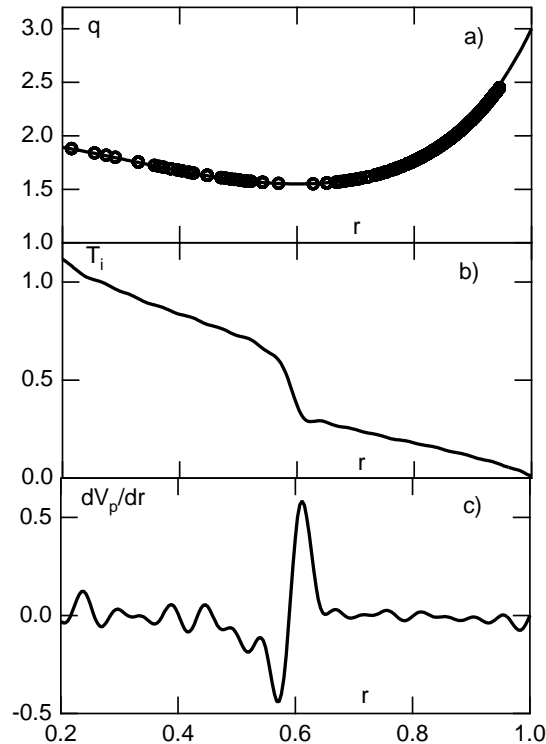


Figure 6: *3D global simulations of ITG turbulence in presence of a magnetic shear reversal. a)  $q$  profile. Points are the positions of resonant surfaces. b) Ion temperature profile. c) Radial profile of the mean  $E \times B$  flow shear.*

In deriving the reduced model, we focus on the 2-D interchange instability system. The interchange modes are unstable when the average magnetic field lines curvature is in opposite direction to the pressure gradient. In the flute approximation, neglecting the stabilizing effect of the sheath conductivity and taking cold ions population, the two dimensional non linear evolution of the normalized density and electric potential is given by:

$$\frac{d}{dt} \nabla_{\perp}^2 \phi = -\frac{g}{n} \frac{\partial n}{\partial y} + \nu \nabla_{\perp}^4 \phi, \quad (3)$$

$$\frac{d}{dt} n = D \nabla_{\perp}^2 n + S. \quad (4)$$

This system is analogous to the Rayleigh-Benard convection with  $n$  standing for the temperature field and  $\phi$  for the stream function.

Let us expand the density and electric potential fields in the following way:

$$n(x, y, t) = \bar{n}(x, t) + \tilde{n}(x, y, t) \quad (5)$$

$$\phi(x, y, t) = \bar{\phi}(x, t) + \tilde{\phi}(x, y, t) \quad (6)$$

where  $\bar{n}$  and  $\bar{\phi}$  are equilibrium quantities averaged along the poloidal direction. The average  $\bar{\phi}$  will further be responsible for the development of a mean flow. So as to reduce the problem to one dimension we expand the poloidal variation of fluctuating quantities in

Fourier series up to the first harmonic of the most unstable mode  $k_y$  (Galerkin projection).

$$\tilde{\phi}(x, y, t) = e^{ik_y y} \phi_1(x, t) + cc \quad (7)$$

$$\tilde{n}(x, y, t) = e^{ik_y y} n_1(x, t) + cc \quad (8)$$

where  $cc$  stands for complex conjugate.

Equations for the evolution of the mean and fluctuating fields read:

$$\partial_t \tilde{n} = -ik \tilde{n} \partial_x \bar{\phi} + ik \tilde{\phi} \partial_x \bar{n} + D \partial_{xx} \tilde{n} \quad (9)$$

$$\partial_t \tilde{\phi} = -ik \tilde{\phi} \partial_x \bar{\phi} + \frac{ig \tilde{n}}{kn_0} + \nu \partial_{xx} \tilde{\phi} \quad (10)$$

$$\partial_t \bar{n} = ik \partial_x (\tilde{n}^* \tilde{\phi} - \tilde{n} \tilde{\phi}^*) + D \partial_{xx} \bar{n} + S \quad (11)$$

$$\partial_t \partial_x \bar{\phi} = ik \partial_x (\tilde{\phi} \partial_x \tilde{\phi}^* - \tilde{\phi}^* \partial_x \tilde{\phi}) + \nu \partial_{xxx} \bar{\phi} \quad (12)$$

We have solved these equations numerically. The source term in the equations is taken gaussian shaped and represents the driving energy sustaining a mean density gradient. In this model, the Reynolds stress is responsible for the generation of a mean zonal flow. Fig. 7 shows the mean velocity profile in which a zoning is observed. By decreasing the dissipation coefficients we were able to increase the number of zones as in Ref. [21]. We observe that propagating bursty events are superimposed to these zonal flows. We found that the latter are necessary to trigger the bursts. In absence of ExB velocity shear, it is impossible to observe large scale transport events in this model.

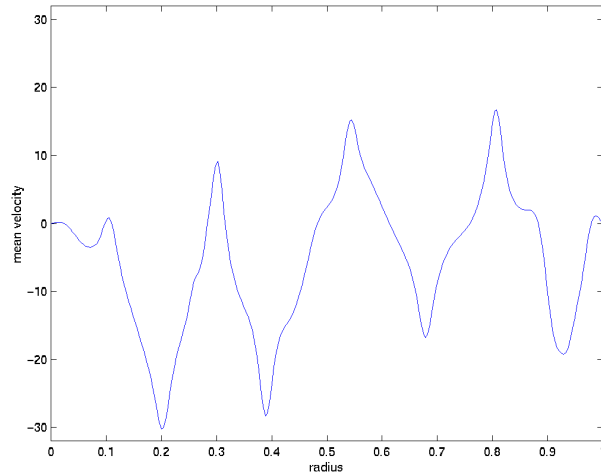


Figure 7: *Time averaged radial velocity profile.*

## Conclusions

Three dimensional simulations of resistive ballooning turbulence at the plasma edge and ITG simulations have shown evidence of large scale transport events. The analysis of the 3D structure of these bursts shows that they are highly radially elongated on the low field side and localized along magnetic field lines. The streamer is found to be generated by an intrinsically nonlinear process. Self generated zonal flows inhibit the growth of bursts, reducing their amplitude and increasing the frequency of appearance. In the presence of a transport barrier generated by a strong shear flow, the amplitudes of bursts almost vanish in the center of the barrier.

## References

- [1] X. Garbet, *et al.*, Nucl. Fusion **39**, 2063 (1999)
- [2] Y. Sarazin, Ph. Ghendrih, Phys. Plasmas **5**, 4214 (1998).
- [3] P. Beyer, *et al.*, Plasma Phys. Control. Fusion **41**, A757 (1999).
- [4] S. Benkadda, *et al.*, Physica Scripta **T84**, 14 (2000).
- [5] F. Jenko, W. Dorland, M. Kotschenreuther, Phys. Plasmas **7**, 1904 (2000).
- [6] P. Beyer, S. Benkadda, X. Garbet, and P.H. Diamond, Phys. Rev. Lett (in press).
- [7] C. Hidalgo, M. A. Pedrosa, B. Ph. van Milligen, E. Sanchez, R. Balbin, I. Garcia-Cortes, J. Bleuel, L. Giannone, H. Niedermeyer, in Fusion Energy 1996 (International Atomic Energy Agency, Vienna, 1997) Vol.1, p.617-624.
- [8] P.A. Politzer, Phys. Rev. Lett. **84**, 1192 (2000).
- [9] B.A. Carreras, B. Ph. van Milligen, M. A. Pedrosa, R. Balbin, C. Hidalgo, D. E. Newman, E. Sanchez *et al.*, Phys. Rev. Lett. **80**, 4438 (1998).
- [10] Y. Sarazin, *et al.*, Phys. Plasmas **7**, 1085 (2000).
- [11] S. Champeaux and P.H. Diamond, submitted.
- [12] J.F. Drake, P.N. Guzdar, A.B. Hassam, Phys. Rev. Lett. **61**, 2205 (1988).
- [13] X. Garbet and R. Waltz, Phys. Plasmas **5**, 2836 (1998).
- [14] P. Beyer and K. H. Spatschek, Phys. Plasmas **3**, 995 (1996).
- [15] P. Beyer, X. Garbet, P. Ghendrih, Phys. Plasmas **5**, 4271 (1998).
- [16] P. Beyer, S. Benkadda, X. Garbet, Phys. Rev. E **61**, 813 (2000).
- [17] B.A. Carreras, *et al.*, Phys. Plasmas **3**, 2903 (1996).
- [18] D.E. Newman, *et al.*, Phys. Plasmas **3**, 1858 (1996).
- [19] P.H. Diamond, T.S. Hahm, Phys. Plasmas **2**, 3640 (1995).
- [20] Y. Sarazin, *et al.*, Proc. 27th EPS Conf. Control. Fusion Plasma Phys. Budapest, Hungary, 2000.
- [21] P. S. Marcus, T. Kundu and Changhoon Lee, Phys. Plasmas **7**, 1630 (2000).